APC Controls Asymmetric Wnt/β-Catenin Signaling and Cardiomyocyte Proliferation Gradient in the Heart

Bo Ye[1,2], **Ning Hou**[1,3], **Lu Xiao**[1], **Yifan Xu**[1], **James Boyer**[1], **Haodong Xu**[4], and **Faqian Li**[1,2,5]

[1]Department of Pathology and Laboratory Medicine, University of Rochester Medical Center, Rochester, NY 14642, USA

[2]Department of Laboratory Medicine and Pathology, University of Minnesota, Room 293, Dwan Variety Club Cardio Research Center, 425 E River Pkwy, Minneapolis, MN 55455

[4]Department of Pathology and Laboratory Medicine, UCLA Center for the Health Science, Room 13-145E, 10833 Le Conte Ave, Los Angeles, CA 90095

Abstract

Aims—Cardiomyocyte (CM) proliferation increases from the inner trabecular to outer compact myocardium in fetal hearts. We determined if canonical Wnt signaling has directional and graded activity to maintain this CM proliferation gradient. Moreover, we investigated whether perturbation of Wnt signaling intensity could modulate CM proliferative activity.

Methods and results—With confocal microscopy and image analysis we found that the Wnt effector, β-catenin, formed a signaling gradient which positively correlated with CM proliferative activity across ventricular walls of wild type (WT) embryos at embryonic day (E) 13.5 and 17.5. Negative Wnt regulators, adenomatosis polyposis coli (APC), had a reverse distribution pattern. The activation of canonical Wnt/β-catenin signaling by deletion of *Apc* in CMs led to ventricular hyperplasia with no adverse effects on fetal survival or CM differentiation. In contrast, cardiac deletion of *β-catenin* resulted in ventricular hypoplasia and fetal demise by E14.5. We further revealed differential distribution and regulation of three cyclin Ds in fetal hearts. Cyclin D1 was mainly expressed in endothelial cells. Although both cyclin D2 and D3 were present in CMs, only cyclin D2 was regulated by Wnt signaling perturbation: downregulation by *β-catenin* deletion and upregulation by Apc knockout.

Conclusion—Canonical Wnt signaling is asymmetrical and graded across ventricular walls and positively regulates CM proliferation via cyclin D2.

[5]**Corresponding Author**: Faqian Li, MD, PhD, MMC 76, Department of Laboratory Medicine and Pathology, C445 Mayor Bldg, 420 Delaware St SE, Minneapolis, MN 55455, USA. Telephone: 612-273-5758. Fax: 612-273-1142. lif@umn.edu.
[3]Current address: Department of Pharmacology, Guangzhou Medical University, Guangzhou, PR China 510182

Graphical Abstract

Keywords

Adenomatosis polyposis coli (APC); β-catenin; heart; development; Wnt; proliferation

1. Introduction

Many signaling pathways including canonical Wnt/β-catenin signaling have been implicated in early heart chamber formation [1, 2], but their roles in the later stages of cardiac development remain poorly defined. During early cardiogenesis, the canonical Wnt/β-catenin pathway regulates various cellular processes, from heart field determination to cardiomyocyte (CM) commitment and differentiation [3]. After heart chambers have formed, CM proliferation increases from the inner trabecular to the outer compact myocardium and is largely responsible for the growth of normal fetal ventricles [4, 5]. How this proliferation gradient is maintained remains poorly understood. It is well documented that canonical Wnt/β-catenin signaling has asymmetric activity during embryonic patterning [6]. Whether this pathway has directional and graded activity in the heart has not been examined in details.

β-Catenin is an important signal transducer in the canonical Wnt/β-catenin pathway [7]. Upon Wnt stimulation, β-catenin is stabilized, enters the nucleus, and binds to transcription factors, including T cell factor/lymphoid enhancer-binding factor (TCF/LEF) family members, which activate target gene transcription [8, 9]. Although disruption of β-catenin in the heart during development is universally lethal, it is controversial and highly debatable whether this canonical regulation of Wnt signaling in β-catenin exists in the heart [3]. Adenomatosis polyposis coli (APC) interacts with β-catenin to form the so called destruction complex including glycogen synthase kinase (GSK)-3β and axin1/2 [3, 7]. GSK-3β phosphorylates β-catenin on serines 33/37 and threonine 41, promoting its degradation

through the ubiquitin/proteasome system. Global deletion of GSK-3β promotes cardiac hyperplasia, but seems to have no major effect on β-catenin stability [10]. On the other hand, chemical inhibition of GSK-3β in cultured neonatal rat CMs enhances proliferation with concomitant β-catenin activation [11].

APC mutation or deletion prevents the formation of this complex and thereby has an essential role in inactivating canonical Wnt signaling [12]. Genetic APC truncation mutations promote β-catenin-mediated signaling and cause colonic adenoma and adenocarcinoma [12, 13]. Germline homozygous *Apc* mutation prevents gastrulation in mice [14] and interferes with cardiac loop morphogenesis in *zebrafish* [15] resulting in excessive endocardial cushions. How *Apc* loss-of-function affects mammalian heart development remains undetermined. Using Cre-Lox technology, we activated and inhibited Wnt signaling through cardiac specific deletion of *Apc* and *β-catenin* respectively. Our data demonstrate that β-catenin is required for CM proliferation. APC deletion activates β-catenin signaling and promotes CM proliferation through the the upregulation of cyclin D2.

2. Methods

2.1 Animals

Mice with two loxP sites inserted in introns 1 and 6 of the *β-catenin* gene were generously donated to the research community by Dr. Rolf Kemler (Max-Planck Institute of Immunology, Germany) (Brault et al, 2001) and maintained at The Jackson Laboratory (Bar Harbor, ME). Mice with two loxP sites flanking the exon 14 of *Apc* [12, 16] were generated by Dr. Tetsuo Noda at The Cancer Institute of Japanese Foundation for Cancer Research (Tokyo, Japan) and acquired from Dr. Bart O. Williams at the Van Andel Research Institute (Grand Rapids, MI, USA). Transgenic mice expressing Cre recombinase under the control of the α-myosin heavy chain promoter *(αMHC-Cre)* were created as previously described [17]. Homozygous *Apc* or *β-catenin* loxP-floxed (*Apc^f/f* or *β-catenin^f/f*) mice were crossed with *αMHC-Cre* mice to generate heterozygous loxP-floxed mice negative for *αMHC-Cre* and positive for αMHC-Cre. Heterozygous loxP-floxed mice positive for αMHC-Cre were bred with homozygous loxP-floxed mice to produce homozygous loxP-floxed or deleted *Apc* and *β-catenin* mice. Pregnant dams were sacrificed via isoflurane inhalation, and then followed by cervical dislocation. Embryos were harvested from the pregnant dam through a hysterectomy at gestational ages between E13.5 to E17.5. Genomic DNA was isolated and purified with DNeasy Blood & Tissue Kit (Qiagen, Valencia, CA). *αMHC-Cre* transgene, loxP-floxed and wild type *β-catenin* genes were amplified by PCR as described previously (Qu J et al, 2007). Analysis for *Apc* alleles was done by multiplex PCR using Apc-P3 primer 5′-GTTCTGTATCATGGAAAGATAGGTGGTC-3′, Apc-P4 primer 5′-CACTCAAAACGCTTTTGAGGGTTGATTC-3′, Apc-P5 primer 5′-GAGTACGGGGTCTCTGTCTCAGTGAA-3′, targeted allele, deleted allele, and wild-type allele amplified as 314-bp (P3 and P4), 258-bp (P3 and P5), and 226-bp (P3 and P4) PCR products, respectively [12, 16]. All procedures were performed in accordance with the Guide for the Care and Use of Laboratory Animals (US Department of Health, Education, and Welfare, Department of Health and Human Services, NIH Publication 85-23), and approved by the University of Rochester Animal Care and Use Committee.

2.2 RNA isolation and RT-PCR

Total RNA was extracted from isolated ventricles of E13.5 and 17.5 embryos using the Trizol reagent from Invitrogen (Life Technologies Corporation, Grand Island, NY) following the manufacturer's instructions. For TaqMan® Assays, real-time RT-PCR was performed with Applied Biosystems 7900HT Sequence Detection System in the Functional Genomics Center of University of Rochester on six pooled ventricles in duplicate with primers for *Axin 2* ordered from Applied Biosystems (Fig. S3C). Data were normalized and standardized with SDS2.2 software provided by Applied System. For custom designed primers (Table S3), real time RT-PCR was performed on at least three different animals in triplicate with MyiQ™ Real-Time PCR Detection System. Results were normalized with *Gapdh* and analyzed with the comparative Ct method. RT-PCR for detecting Apc deletion was carried out with the DreamTaq Green Buffer (Life Technologies Corporation, Grand Island, NY) and visualized with 3% agarose gels using F546 primer 5′-TGAGGAATTTGTCTTGGCGAG-3′ and R721 primer 5′-GCACTTCCCATGGCAATCATT-3′.

2.3 Histology and immunohistochemistry

Murine hearts were fixed in 4% paraformaldehyde at room temperature for 30 min and embedded in paraffin. Four μm sections were used for hematoxylin and eosin or immunohistochemical staining as previously described[18]. Antigen retrieval was performed in EDTA buffer (pH: 9.0) by heating to 99°C for 20 minutes with a PT Link system from Dako (Carpinteria, CA). Endogenous peroxidase activity was quenched with 3% hydrogen peroxide and non-specific binding was blocked with 10% non-immune goat serum (Invitrogen, Carlsbad, CA). Primary antibodies (Table S5) were incubated overnight in a moisturized chamber at 4°C. The signal was amplified with the Histostain-SP Kit (Life Technologies Corporation, Grand Island, NY) according to manufacturer's instruction.

2.4 Immunofluorescent labeling and confocal microscopy

Paraformaldehyde-fixed hearts were washed with PBS and immersed in 30% sucrose/PBS for 30 min to 1 hour and then embedded with O.C.T compound. Five μm sections were washed with 0.1 mol/L glycine for 25 min in order to reduce non-specific crosslinking activity of residual paraformaldehyde, immersed in 10% normal goat serum for 60 min to block non-specific binding, and then incubated overnight at 4°C with primary antibodies (Table S5). After washing 6 times with PBS, secondary antibody labeled with DyLight-555 or 488 (Life Technologies Corporation, Grand Island, NY) was added. Nuclear counterstain was performed with 4′, 6-Diamidino-2-Phenylindole (DAPI, Sigma-Aldrich, St. Louis, MO). Confocal images were collected with Olympus FV1000 confocal microscope (Olympus America Inc., Melville, NY) under uniform settings. For negative controls, primary antibodies were omitted or substituted with rabbit serum under the same conditions.

2.5 Quantification of fluorescent intensity and measurement of ventricular wall thickness

Five μm frozen sections were labeled with β-catenin, APC and costained with sarcomeric α-actinin (Actinin) and DAPI. Ventricles were scanned at 40× and 0.55 μm z-intervals with an Olympus FV1000 confocal microscope. Five sequential images along the z-axis were

stacked to generate a merged image for further intensity quantification by ImageJ (Fiji). The intensity of β-catenin and APC was measured in all Actinin positive regions of 40× magnification images, and presented as the mean fluorescence intensity in pixels. The mean nuclear pixel intensity of β-catenin was measured in DAPI stained CM nuclei of all Actinin positive regions at 40× (Fig. 1G).

Compact layer thickness was perpendicularly measured from the epicardium to the junction of compact and trabecular layers in the Actinin positive region at five random locations from three sections per heart.

2.6 SDS gel electrophoresis and Western blotting

Isolated ventricles from E17.5 hearts were collected and extracted with RIPA buffer (Life Technologies Corporation, Grand Island, NY). An equal amount of total protein, determined with the Bio-Rad Coomassie Protein Assay (Bio-Rad Laboratories, Hercules, CA) from each group, was loaded and separated by 4-12% NuPAGE® Bis-Tris Pre-Cast gels (Life Technologies Corporation, Grand Island, NY). Target proteins were detected with specific antibodies using SuperSignal™ West Pico Chemiluminescent Substrate (Thermo, Rockford, IL). Protein band intensity was quantified with NIH ImageJ software (http://rsb.info.nih.gov/ij/) using relative densitometric values on the duplicates of at least three independent experiments from each group.

2.7 Statistics

Fluorescent intensity and real time RT-PCR data were presented as mean ± standard deviation (SD) of the mean. Means among groups were analyzed with SPSS 13.0 software (IBM Corporation, Armonk, NY) using Independent-Sample T Test for two groups and One-Way ANOVA for more than two groups. Post hoc multiple comparisons were then performed to determine if a statistical significance was detected between groups. Fisher's least significant difference (LSD) was used to compare group means when equal variances were present. If equal variances were not assumed, differences between group means were calculated by Tamhane's T2 test.

3. Results

3.1 Canonical Wnt signaling gradient correlates with CM proliferative activity

CMs show a proliferation gradient across the ventricular wall with the highest proliferation rate at the epicardial compact layer of embryonic hearts [4]. A recent report revealed that proliferating CMs that are often seen at the compact layer are positive for active nuclear β-catenin, indicating Wnt signaling intensity may control cardiac proliferation [19]. In the intestines, Wnt signaling intensity correlates with the proliferative activity from the base of crypt to the surface epithelial cells [20, 21]. We wondered whether canonical Wnt/β-catenin signaling also formed similar signaling gradient across the ventricular wall to regulate CM proliferation. We found that Wnt signaling components did indeed show graded and directional distribution in the ventricular wall of wild type (WT) embryos at embryonic day (E) 13.5 (Fig. 1). The Wnt effector β-catenin had an intensity gradient with the highest level at the epicardial compact layer (Fig. 1A) corresponding to CM proliferation activity reveled

by Ki67 (Fig. 1C and D). Although β-catenin is predominantly membranous (Fig 1B), its nuclear signals were clearly detected at higher magnification (Fig. S1A), with a similar intensity gradient (Fig. 1G, bar graph) to that of total β-catenin (Fig. 1B, bar graph) from the outer to inner layer across the ventricular wall. Reversely, the Wnt suppressor APC (Fig. 1E and F) demonstrated the strongest intensity at the innermost trabecular layer.

3.2 Cardiac *β-catenin* deletion inhibited CM proliferation

The α-myosin heavy chain (*αMHC*) is transiently expressed in differentiating CMs during cardiac chamber formation from E10.5 to 14.5 [22] and *αMHC* promoter driven Cre recombinase (*αMHC-Cre*) can be used to delete loxP floxed genes, specifically in fetal CMs [17]. To elucidate the cell-autonomous role of β-catenin in CMs, we introduced *αMHC-Cre* into mice with loxP sites inserted in introns 1 and 6 of the *β-catenin* gene (*β-Cat^f*)[23] to specifically delete *β-catenin* in CMs. Compared to WT (*β-Cat^{f/+};αMHC-Cre^−*) or heterozygous *β-catenin* deletion (*β-Cat^{f/+};αMHC-Cre^+*) siblings (Fig. 2A and 2B), β-catenin was significantly reduced in homozygous *β-catenin* conditional knockout (*β-Cat^{f/f};αMHC-Cre^+=β-Cat* cKO) mice in protein (Fig. 2C and 2D) and mRNA levels (Fig. 2G) by E13.5. *Rosa*^{mT/mG} reporter mice for Cre activity revealed efficient conversion of red to green membrane-targeted signals by *αMHC-Cre* in both compact and trabecular layers at E13.5 (Fig. S1B). As reported previously, heterozygous loss of *β-catenin* in CMs had no detectable effects on mouse development and no homozygous *β-catenin* deleted mice were detected at birth [24]. No gross or histologic abnormality was observed at E10.5 and E11.5 in *β-Cat* cKO mice. Embryos with *β-Cat* cKO were also grossly unremarkable at E12.5, but had slight expansion of the pericardial space, indicating pericardial edema. At 13.5, all genotypes were present at the expected numbers (Table S1). A small percentage of *β-Cat* cKO embryos (4 out of 18) were grossly pale and microscopically necrotic, consistent with autolysis. The remaining littermates (14 out of 18) were grossly normal (Fig. S2A), but shown signs of congestive heart failure with pericardial edema (Fig. S2B and S2C). Hearts were smaller with thinner left and right ventricular walls in *β-Cat* cKO embryos compared to that of *β-Cat^{f/+};αMHC-Cre^−* WT controls (Fig. 2N and Fig. 2O, upper panel). β-Catenin was significantly reduced in CMs at both compact and trabecular layers, resulting in the loss of normal β-catenin signaling gradient along the ventricular wall (Fig 2C and 2D). Consistent with our hypothesis, Ki67 positive CMs decreased more than 50% in the compact layer from 43.0% in WT to 19.7% in *β-Cat* cKO mice at E13.5. The trabecular layer had low proliferative activity and less β-catenin than the compact layer in normal embryos (Fig. 2O, lower panel and Fig. 2P). Thus, β-catenin deletion had less significant impact on Ki67 labeling in the trabecular layer. pH3S10 (Fig. S3A and S3B) were also reduced in CMs of *β-Cat* cKO compared to WT embryos. On the other hand, APC intensity gradient remained intact in *β-Cat* cKO ventricles (Fig. 2J and K) similar to WT controls (Fig. 2 H and I). There was a slight increase in APC at the compact layer, but no statistical significance was detected by quantitative confocal microscopy (Fig. 2L). Real-time RT-PCR also did not reveal statistical significance in *Apc* mRNA levels between cKO and WT groups (Fig. 2M). No increase in apoptosis was detected by TUNEL labeling and anti-cleaved active caspase 3 staining in the heart of *β-Cat* cKO embryos at E13.5 (Fig. S2D). At E14.5, *β-Cat* cKO embryos were reduced in numbers (Table S1) and demonstrated autolysis and absorption.

These findings suggest that β-catenin is required for normal cardiac development and necessary to maintain higher proliferation rate in the compact layer.

3.3 Cardiac *Apc* deletion promotes CM proliferation

Adenomatosis polyposis coli (APC) suppresses canonical Wnt signaling by promoting β-catenin degradation and its germline homozygous *Apc* mutation impairs cardiac loop morphogenesis in *zebrafish* [15] resulting in excessive endocardial cushions. How *Apc* loss-of-function affects mammalian heart development remains undetermined. We employed *αMHC-Cre* to delete *Apc* in fetal CMs with a well-characterized mouse model containing LoxP sites flanked at the exon 14 of the *Apc* gene (*Apc^f*) [12, 16]. Genomic PCR and RT-PCR demonstrated that *αMHC-Cre* mediated cardiac-specific excision of exon 14 (Fig. S4). All genotypes were present at expected numbers (Table S2). Embryos with homozygous *Apc* deletion (*Apc$^{f/f}$;αMHC-Cre$^+$= Apc* cKO) showed normal morphology from E13.5 to E17.5 compared with *Apc$^{f/+}$; αMHC-Cre$^-$* (*Apc* WT) control embryos. Hearts from *Apc* cKO embryos were larger and had thicker ventricular walls at E13.5 (Fig. 3J and 3K, upper panel) and at E17.5 (Fig 4A) compared to their WT siblings. As expected, APC gradient was disrupted and APC expression was dramatically reduced in the heart in *Apc* cKO embryos at E13.5 and E17.5 (Fig.3E and Fig.S5B). Consequently, β-catenin was increased in the heart and accumulated in the nucleus of CMs in *Apc* cKO mice E13.5 (Fig. 3F2) and E17.5 (Fig. S5B1 and S5B2). Western blots demonstrated the reduction of APC and accumulation of β-catenin in *Apc* cKO hearts (Fig. S6). Proliferation activity of CMs as indicated by Ki67 increased 36% in compact layer and 50% in trabecular layers over WT littermates at E13.5 respectively (Fig. 3K, lower panel and 3L). This increase continued to E17.5 by 42% in the compact layer and 52% in the trabecular layer (Fig. 4B and 4C, lower panel) in *Apc* cKO embryos over their WT siblings. pH3S10 also revealed an increase in in *Apc* cKO CMs at E13.5 (Fig. S3A and S3B) and E17.5 (Fig. 4B and 4C, upper panel). These results indicate that APC with higher expression level in the inner trabecular layer is an important repressor of canonical Wnt/β-catenin signaling in the heart to inhibit CM proliferation.

3.4 Genetic interaction of *β-catenin* with *Apc*

To dissect the genetic interaction of APC with β-catenin in CMs during later stage of heart development, we generated *Apc and β-catenin* compound deletion mice. The loss of one copy of *β-catenin* dampened the effect of *Apc* cKO on CM proliferation (Fig 4C) and β-catenin signaling (Fig. S5C) at E17.5. This result indicates that β-catenin is a downstream effector regulated by APC. On the other hand, one or two copy loss of *Apc* could only partially extend the survival of *β-Cat* cKO embryos from E14.5 to E17.5 (Fig. S4E). By this age, *Apc* deletion could not prevent the loss of β-catenin signaling across the ventricle (Fig. S5D and S5E) in *β-Cat* cKO embryos. These findings are consistent with the role of APC in β-catenin stability [13]. Consequently, β-catenin degrades slower and has a longer half-life in *β-catenin*/*Apc* double than in *β-catenin* single cKO mutants. Therefore, *β-catenin*/*Apc* double mutants live slightly longer than *β-catenin* single mutants.

3.5 Wnt target and cell cycle gene expression by *β-catenin* and *Apc* deletion

Axin2 is ubiquitously expressed in many tissues and is considered a universal target of canonical Wnt pathway [25]. By real-time RT PCR, *Axin2* transcripts were increased by 4.5-fold in *Apc* cKO mice and decreased by 70% in *β-Cat* cKO mice at E13.5 (Fig. S3C), indicating canonical Wnt signaling is regulated by APC and β-catenin in the heart. D-type cyclins and c-myc are among the earliest identified canonical Wnt targets [26-29]. Upregulation of c-*myc* was identified in *Apc* cKO mice, but its downregulation was not detected in *β-Cat* cKO mice at E13.5 (Fig. 6A and Table S4). Additionally, no significant increase of c-*myc* was observed in *Apc* cKO mice at E17.5 (Fig. 6B). Although *Cyclin D1* is a clear target in *Apc* mutant tumor cells [27, 28], only *Cyclin D2* was immediately induced by *Apc* loss-of-function in colon [29]. Our data demonstrated that the expression levels of *Cyclin D1* and *Cyclin D3* were not changed in either *Apc* or *β-catenin* deleted hearts at E13.5 (Fig. 5A and 5E) or E17.5 (Fig. 5B and 5F). In contrast, *Cyclin D2* mRNA levels were significantly increased in *Apc* cKO hearts at E13.5 (Fig. 5E) and E17.5 (Fig. 5F), and decreased in *β-Cat* cKO mice at E17.5 (Fig. 6B). Similarly, only cyclin D2, but not D1 and D3 proteins were elevated in at E17.5 (Fig. S6). However, *cyclin D2* mRNA was only slightly, but not statistically significantly decreased in *β-Cat* cKO mice at E13.5 (Fig. 5E) partially due to its high expression in endothelial cells. Interestingly, cyclin D1 was mainly expressed in endothelial cells while cyclin D2 and D3 were detected in both CMs and endothelial cells (Fig. 5A-D). Again, only cyclin D2 was increased in CMs of *Apc* cKO mice and decreased (Fig. 5C) in *β-Cat* cKO mice by immunofluorescent staining. In parallel, protein levels of proliferation markers: Ki67 and pH3S10 were elevated in *Apc* cKO at E17.5 (Fig. S6).

3.6 Wnt signaling perturbation on cardiac gene expression

In many cell types, the proliferation rate is tightly correlated with differentiation status. In zebrafish, global loss of APC function has been shown to promote CM proliferation, but inhibit maturation[15]. We examined the expression of *Gata4, Hand1, Hand2, Myh6, Myh7, Myl2, Myl7, Nppa* (ANF), Nkx2.5, Pdgfra, SMA, Tbx2, Tbx3, Tbx5, Tbx18, Tbx20 and *WT1* by real time RT-PCR (Fig. 6A and Table S4). *Hand1, Hand2, Myh7, Myl7, Nppa, SMA, Tbx3* and *Tbx5* were upregulated while *Myh6, Tbx2* and *Tbx18* were downregulated by cardiac *Apc* deletion. However, these changes were less than 40% among different genotypes except *Nppa* and *Myl7*. These results suggest that Wnt signaling mainly regulate cardiac proliferation rather than differentiation after E13.5.

4. Discussion

The role of canonical Wnt signaling in cardiac development remains controversial and needs to be further defined with genetic manipulation of key signaling molecules in a cell and developmental stage specific manner. In *Drosophila* and mice, canonical Wnt/β-catenin signaling is required for cardiac field specification and morphogenesis [30]. On the other hand, cardiogenesis in gastrulating amphibians and chicks requires canonical Wnt/β-catenin signaling inhibition [31, 32]. A biphasic role, stimulatory before and inhibitory during and after gastrulation, has therefore been stipulated for the canonical Wnt pathway in cardiogenesis [33]. However, this proposed inhibitory effect after gastrulation is contradicted

by the fact that *β-catenin* deletion in cardiac progenitor cells and their differentiated descendants through Cre driven by several cardiac promoters such as *Isl1, Mef2c, MesP1, Nkx2.5,* or *SM22α* impairs cardiac development and fetal survival [34-37]. The activity of these promoters in migrating cardiac committed cells as well as their offspring settling in the heart proper makes it difficult to distinguish the roles of canonical Wnt/β-catenin signaling in cell migration, differentiation, and proliferation of cardiac lineage cells. Additionally, the embryonic lethality of these models prevented exploring how β-catenin-mediated canonical Wnt signaling regulates cardiac chamber maturation and CM expansion after cardiac looping morphogenesis. Through genetic deletion of Apc/β-catenin by *αMHC-Cre*, we have shown that APC controls asymmetrical Wnt signaling across ventricular walls and suppresses β-catenin activity in the trabecular layer. Conversely, high β-catenin levels are essential for CM proliferation and normal ventricular maturation.

4.1 Canonical Wnt signaling gradient and cell proliferation

After cardiac chamber morphogenesis and initial four chamber formation, CMs proliferate rapidly for ventricular compaction and septation [4]. Closer to the birth, CM cell cycle activity decreases significantly [5]. A second wave of DNA replication occurs during first 2 weeks after birth, resulting in CM binucleation, but not cell division [5]. Global and regional deficiency in CM proliferation can lead to ventricular septal defect and non-compaction. Therefore, CM cell cycle regulation is essential to understand normal ventricular maturation. We have confirmed that CM proliferation forms a decreasing gradient from the outer to the inner myocardium [4]. More importantly, we have revealed that negative Wnt regulator APC is mainly expressed at the inner trabecular layer while Wnt nuclear β-catenin effector has the highest level at the outer compact myocardium. Similarly, Buikema et al have reported that there are more nuclear active positive CMs in the compact than trabecular layer [19]. These findings indicate that canonical Wnt/β-catenin has directional and graded activity across the ventricular wall to regulate CM proliferation. It is well known that canonical Wnt/β-catenin signaling has asymmetric activity and directional signaling during development [6]. Wnt signaling intensity has also been reported to correlate with the proliferative activity from the base of the crypt to the surface epithelial cells of the intestines [20, 21].

4.2 Canonical Wnt signaling promotes and is required for CM proliferation after chamber formation

Our results have shown that CM cannot proliferate sufficiently to build normal ventricles without β-catenin. On the other hand, Wnt activation by cardiac *Apc* deletion promotes CM proliferation without significant effect on CM differentiation in late embryonic development. Similarly, Wnt signaling activation and inhibition in CMs expressing myosin light chain (MlC) 2v which is a ventricular form of MLC2 [38] demonstrate that β-catenin stabilization by deleting its exon 3 enhances CM cell cycle activity [19]. Global and cardiac specific deletion of GSK-3β which negatively regulates stability also promotes CM proliferation in neonatal and adult hearts [10, 39]. These results indicate that canonical Wnt signaling can promote CM proliferation and is required for cardiac chamber maturation during embryonic development.

4.3 Wnt signaling regulates cell cycle gene expression

All three type of cyclin Ds are expressed in the heart [5]. However, cyclin D1 is not detected by Western blotting in CMs isolated from neonatal hearts [40]. Our localization study confirms that cyclin D1 is expressed in endothelial cells, but not CMs at E13.5 and E17.5. In addition, cyclin D1 expression is not affected by cardiac Wnt activation and inhibition. Cyclin D3 is equally expressed in CMs and endothelial cells, and shows no significant change upon Wnt activation and inhibition. In WT embryos, more cyclin D2 is present in endothelial cells than CMs. Cardiac Wnt activation by *Apc* deletion increases cyclin D2 in CMs, but not endothelial cells. Conversely, cardiac *β-catenin* deletion decreases cyclin D2 expression in CMs. Stabilizing β-catenin in CMs before E13.5 has been previously shown to enhance cyclin D2 expression [41, 42]. Moreover, cyclin D2 overexpression is more effective to promote CM proliferation than cyclin D1 and D3 overexpression after cardiac injury [43]. All these findings indicate that cyclin D2 is the most significantly affected one of all 3 cyclin Ds by cardiac Wnt signaling manipulation and may have important roles in CM cell cycle regulation during all stages of heart development and in cardiac repair after damage.

4.4 Cell autonomous vs cell non-autonomous cell cycle control

The roles of canonical Wnt/β-catenin signaling in cardiogenesis are dependent on the developmental stage and cellular context [3]. Before gastrulation, canonical Wnt/β-catenin signaling promotes cardiac commitment and differentiation in many species. In contrast, differential effects of this pathway on CM expansion have been reported among mice, zebrafish, amphibians, and chicks after gastrulation. Conditional deletion and transgenic overexpression of Wnt signaling component in this study and previous investigations [19, 42] have demonstrated that this pathway enhances and is necessary for CM expansion in mice after gastrulation. On the other hand, several studies have indicated that cardiogenesis in zebrafish, amphibians and chicks requires Wnt signaling inhibition after gastrulation [31, 32, 44]. In the chick, posterior lateral plate mesoderm normally forms blood, but Wnt inhibition induces cardiac specific gene expression from this tissue [31]. Similarly, Wnt suppression can induce cardiogenesis in explants from noncardiogenic ventral marginal zone mesoderm in *Xenopus laevis* [32]. Global Wnt activation also inhibits heart specification after gastrulation in *Zebrafish* [44]. Nevertheless, these experiments with Wnt manipulation in intact animal, organ culture, or tissue implants could not separate cell autonomous vs non-cell autonomous effect. This cell vs non-cell autonomous difference in CM proliferation has also been observed in retinoid acid signaling [45]. Global deficiency in retinoid acid receptor RXRα causes ventricular hypoplasia while cardiac specific deletion of RXRα has not significant impact on normal cardiac development. With cardiac specific Wnt activation and inhibition, we have shown that the cell autonomous role of canonical Wnt/beta-catenin signaling in CMs is to promote rather than inhibit CM expansion after looping morphogenesis. Therefore, Wnt stimulation could be explored to strengthen ventricular development in patients with ventricular hypoplasia, promote cardiac regeneration in vivo, and expand differentiated CMs in vitro.

Supplementary Material

Refer to Web version on PubMed Central for supplementary material.

Acknowledgements

Abbreviations

APC	adenomatosis polyposis coli
cKO	conditional knockout
CM	cardiomyocyte
E	embryonic day
WT	wild type

References

[1]. Hurlstone AFL, Haramis A-PG, Wienholds E, Begthel H, Korving J, van Eeden F, et al. The Wnt/[beta]-catenin pathway regulates cardiac valve formation. Nature. 2003; 425:633–7. [PubMed: 14534590]

[2]. Olson EN. Gene Regulatory Networks in the Evolution and Development of the Heart. Science. 2006; 313:1922–7. [PubMed: 17008524]

[3]. Cohen ED, Tian Y, Morrisey EE. Wnt signaling: an essential regulator of cardiovascular differentiation, morphogenesis and progenitor self-renewal. Development. 2008; 135:789–98. [PubMed: 18263841]

[4]. Sedmera D, Reckova M, DeAlmeida A, Coppen SR, Kubalak SW, Gourdie RG, et al. Spatiotemporal pattern of commitment to slowed proliferation in the embryonic mouse heart indicates progressive differentiation of the cardiac conduction system. The Anatomical Record Part A: Discoveries in Molecular, Cellular, and Evolutionary Biology. 2003; 274A:773–7.

[5]. Soonpaa MH, Kim KK, Pajak L, Franklin M, Field LJ. Cardiomyocyte DNA synthesis and binucleation during murine development. American Journal of Physiology - Heart and Circulatory Physiology. 1996; 271:H2183–H9.

[6]. Larabell CA, Torres M, Rowning BA, Yost C, Miller JR, Wu M, et al. Establishment of the dorso-ventral axis in Xenopus embryos is presaged by early asymmetries in beta-catenin that are modulated by the Wnt signaling pathway. J Cell Biol. 1997; 136:1123–36. [PubMed: 9060476]

[7]. Miller JR, Moon RT. Signal transduction through beta-catenin and specification of cell fate during embryogenesis. Genes Dev. 1996; 10:2527–39. [PubMed: 8895655]

[8]. Behrens J, von Kries JP, Kuhl M, Bruhn L, Wedlich D, Grosschedl R, et al. Functional interaction of beta-catenin with the transcription factor LEF-1. Nature. 1996; 382:638–42. [PubMed: 8757136]

[9]. Grigoryan T, Wend P, Klaus A, Birchmeier W. Deciphering the function of canonical Wnt signals in development and disease: conditional loss- and gain-of-function mutations of {beta}-catenin in mice. Genes Dev. 2008; 22:2308–41. [PubMed: 18765787]

[10]. Kerkela R, Kockeritz L, Macaulay K, Zhou J, Doble BW, Beahm C, et al. Deletion of GSK-3beta in mice leads to hypertrophic cardiomyopathy secondary to cardiomyoblast hyperproliferation. J Clin Invest. 2008; 118:3609–18. [PubMed: 18830417]

[11]. Tseng A-S, Engel FB, Keating MT. The GSK-3 Inhibitor BIO Promotes Proliferation in Mammalian Cardiomyocytes. Chemistry & Biology. 2006; 13:957–63. [PubMed: 16984885]

[12]. Shibata H, Toyama K, Shioya H, Ito M, Hirota M, Hasegawa S, et al. Rapid colorectal adenoma formation initiated by conditional targeting of the Apc gene. Science. 1997; 278:120–3. [PubMed: 9311916]

[13]. Su LK, Vogelstein B, Kinzler KW. Association of the APC tumor suppressor protein with catenins. Science. 1993; 262:1734–7. [PubMed: 8259519]

[14]. Fodde R, Edelmann W, Yang K, van Leeuwen C, Carlson C, Renault B, et al. A targeted chain-termination mutation in the mouse Apc gene results in multiple intestinal tumors. Proceedings of the National Academy of Sciences of the United States of America. 1994; 91:8969–73. [PubMed: 8090754]

[15]. Hurlstone AF, Haramis AP, Wienholds E, Begthel H, Korving J, Van Eeden F, et al. The Wnt/beta-catenin pathway regulates cardiac valve formation. Nature. 2003; 425:633–7. [PubMed: 14534590]

[16]. Cole AM, Myant K, Reed KR, Ridgway RA, Athineos D, Van den Brink GR, et al. Cyclin D2-cyclin-dependent kinase 4/6 is required for efficient proliferation and tumorigenesis following Apc loss. Cancer Res. 2010; 70:8149–58. [PubMed: 20736363]

[17]. Agah R, Frenkel PA, French BA, Michael LH, Overbeek PA, Schneider MD. Gene recombination in postmitotic cells. Targeted expression of Cre recombinase provokes cardiac-restricted, site-specific rearrangement in adult ventricular muscle in vivo. J Clin Invest. 1997; 100:169–79. [PubMed: 9202069]

[18]. Yi XP, Gerdes AM, Li F. Myocyte redistribution of GRK2 and GRK5 in hypertensive, heart-failure-prone rats. Hypertension. 2002; 39:1058–63. [PubMed: 12052842]

[19]. Buikema JW, Mady AS, Mittal NV, Atmanli A, Caron L, Doevendans PA, et al. Wnt/β-catenin signaling directs the regional expansion of first and second heart field-derived ventricular cardiomyocytes. Development. 2013; 140:4165–76. [PubMed: 24026118]

[20]. Gregorieff A, Pinto D, Begthel H, Destrée O, Kielman M, Clevers H. Expression Pattern of Wnt Signaling Components in the Adult Intestine. Gastroenterology. 2005; 129:626–38. [PubMed: 16083717]

[21]. Angus-Hill ML, Elbert KM, Hidalgo J, Capecchi MR. T-cell factor 4 functions as a tumor suppressor whose disruption modulates colon cell proliferation and tumorigenesis. Proceedings of the National Academy of Sciences. 2011; 108:4914–9.

[22]. Zammit PS, Kelly RG, Franco D, Brown N, Moorman AF, Buckingham ME. Suppression of atrial myosin gene expression occurs independently in the left and right ventricles of the developing mouse heart. Dev Dyn. 2000; 217:75–85. [PubMed: 10679931]

[23]. Brault V, Moore R, Kutsch S, Ishibashi M, Rowitch DH, McMahon AP, et al. Inactivation of the beta-catenin gene by Wnt1-Cre-mediated deletion results in dramatic brain malformation and failure of craniofacial development. Development. 2001; 128:1253–64. [PubMed: 11262227]

[24]. Qu J, Zhou J, Ping Yi X, Dong B, Zheng H, Miller LM, et al. Cardiac-specific haploinsufficiency of β-catenin attenuates cardiac hypertrophy but enhances fetal gene expression in response to aortic constriction. Journal of Molecular and Cellular Cardiology. 2007; 43:319–26. [PubMed: 17673255]

[25]. Lustig B, Jerchow B, Sachs M, Weiler S, Pietsch T, Karsten U, et al. Negative Feedback Loop of Wnt Signaling through Upregulation of Conductin/Axin2 in Colorectal and Liver Tumors. Mol Cell Biol. 2002; 22:1184–93. [PubMed: 11809809]

[26]. He TC, Sparks AB, Rago C, Hermeking H, Zawel L, da Costa LT, et al. Identification of c-MYC as a target of the APC pathway [see comments]. Science. 1998; 281:1509–12. [PubMed: 9727977]

[27]. Shtutman M, Zhurinsky J, Simcha I, Albanese C, D'Amico M, Pestell R, et al. The cyclin D1 gene is a target of the beta-catenin/LEF-1 pathway. Proc Natl Acad Sci U S A. 1999; 96:5522–7. [PubMed: 10318916]

[28]. Tetsu O, McCormick F. [beta]-Catenin regulates expression of cyclin D1 in colon carcinoma cells. Nature. 1999; 398:422–6. [PubMed: 10201372]

[29]. Sansom OJ, Reed KR, Hayes AJ, Ireland H, Brinkmann H, Newton IP, et al. Loss of Apc in vivo immediately perturbs Wnt signaling, differentiation, and migration. Genes Dev. 2004; 18:1385–90. [PubMed: 15198980]

[30]. Cohen ED, Tian Y, Morrisey EE. Wnt signaling: an essential regulator of cardiovascular differentiation, morphogenesis and progenitor self-renewal. Development. 2008; 135:789–98. [PubMed: 18263841]

[31]. Marvin MJ, Di Rocco G, Gardiner A, Bush SM, Lassar AB. Inhibition of Wnt activity induces heart formation from posterior mesoderm. Genes Dev. 2001; 15:316–27. [PubMed: 11159912]

[32]. Schneider VA, Mercola M. Wnt antagonism initiates cardiogenesis in Xenopus laevis. Genes Dev. 2001; 15:304–15. [PubMed: 11159911]

[33]. Ueno S, Weidinger G, Osugi T, Kohn AD, Golob JL, Pabon L, et al. Biphasic role for Wnt/beta-catenin signaling in cardiac specification in zebrafish and embryonic stem cells. Proc Natl Acad Sci U S A. 2007; 104:9685–90. [PubMed: 17522258]

[34]. Kwon C, Arnold J, Hsiao EC, Taketo MM, Conklin BR, Srivastava D. Canonical Wnt signaling is a positive regulator of mammalian cardiac progenitors. Proc Natl Acad Sci U S A. 2007; 104:10894–9. [PubMed: 17576928]

[35]. Ai D, Fu X, Wang J, Lu MF, Chen L, Baldini A, et al. Canonical Wnt signaling functions in second heart field to promote right ventricular growth. Proc Natl Acad Sci U S A. 2007; 104:9319–24. [PubMed: 17519332]

[36]. Klaus A, Saga Y, Taketo MM, Tzahor E, Birchmeier W. Distinct roles of Wnt/beta-catenin and Bmp signaling during early cardiogenesis. Proc Natl Acad Sci U S A. 2007; 104:18531–6. [PubMed: 18000065]

[37]. Cohen ED, Wang Z, Lepore JJ, Lu MM, Taketo MM, Epstein DJ, et al. Wnt/beta-catenin signaling promotes expansion of Isl-1-positive cardiac progenitor cells through regulation of FGF signaling. J Clin Invest. 2007; 117:1794–804. [PubMed: 17607356]

[38]. Chen J, Kubalak SW, Minamisawa S, Price RL, Becker KD, Hickey R, et al. Selective Requirement of Myosin Light Chain 2v in Embryonic Heart Function. Journal of Biological Chemistry. 1998; 273:1252–6. [PubMed: 9422794]

[39]. Woulfe KC, Gao E, Lal H, Harris D, Fan Q, Vagnozzi R, et al. Glycogen Synthase Kinase-3{beta} Regulates Post-Myocardial Infarction Remodeling and Stress-Induced Cardiomyocyte Proliferation In Vivo. Circ Res. 2010; 106:1635–45. [PubMed: 20360256]

[40]. Poolman RA, Brooks G. Expressions and Activities of Cell Cycle Regulatory Molecules During the Transition from Myocyte Hyperplasia to Hypertrophy. Journal of Molecular and Cellular Cardiology. 1998; 30:2121–35. [PubMed: 9799664]

[41]. Ai D, Fu X, Wang J, Lu M-F, Chen L, Baldini A, et al. Canonical Wnt signaling functions in second heart field to promote right ventricular growth. PNAS. 2007; 104:9319–24. %R 101073/pnas0701212104. [PubMed: 17519332]

[42]. Kwon C, Arnold J, Hsiao EC, Taketo MM, Conklin BR, Srivastava D. Canonical Wnt signaling is a positive regulator of mammalian cardiac progenitors. Proceedings of the National Academy of Sciences. 2007; 104:10894–9.

[43]. Pasumarthi KBS, Nakajima H, Nakajima HO, Soonpaa MH, Field LJ. Targeted Expression of Cyclin D2 Results in Cardiomyocyte DNA Synthesis and Infarct Regression in Transgenic Mice. Circ Res. 2005; 96:110–8. [PubMed: 15576649]

[44]. Ueno S, Weidinger G, Osugi T, Kohn AD, Golob JL, Pabon L, et al. From the Cover: Biphasic role for Wnt/beta-catenin signaling in cardiac specification in zebrafish and embryonic stem cells. Proceedings of the National Academy of Sciences. 2007; 104:9685–90.

[45]. Chen J, Kubalak SW, Chien KR. Ventricular muscle-restricted targeting of the RXRalpha gene reveals a non-cell-autonomous requirement in cardiac chamber morphogenesis. Development. 1998; 125:1943–9. [PubMed: 9550726]

Highlights

1)   β-cat played a critical role in maintaining CM proliferation gradient.

2)   APC formed an intensity gradient opposite to β-cat and CM proliferative activity.

3)   With Apc/β-cat double cKO, we found that Wnt signaling regulated cyclin D2.
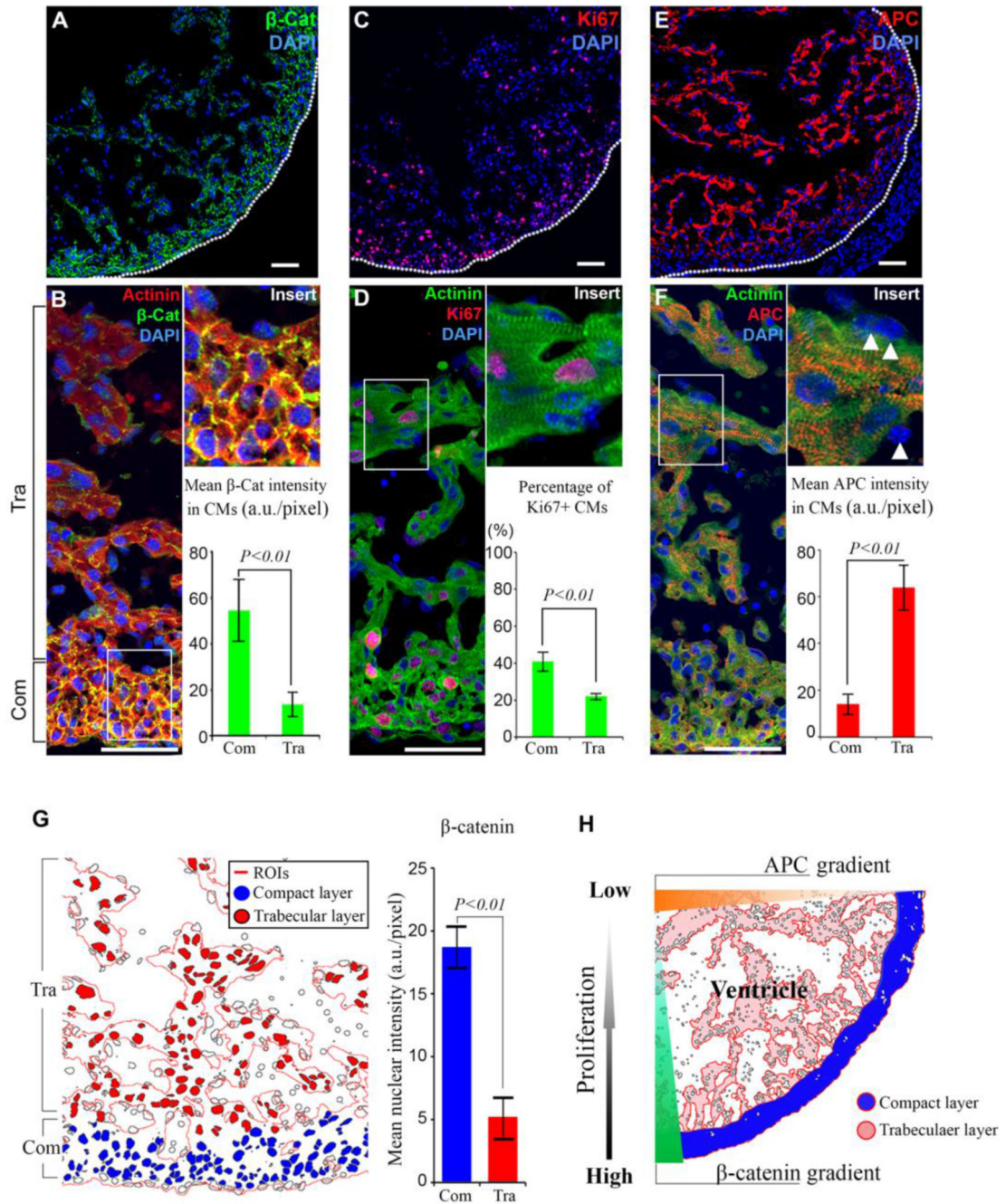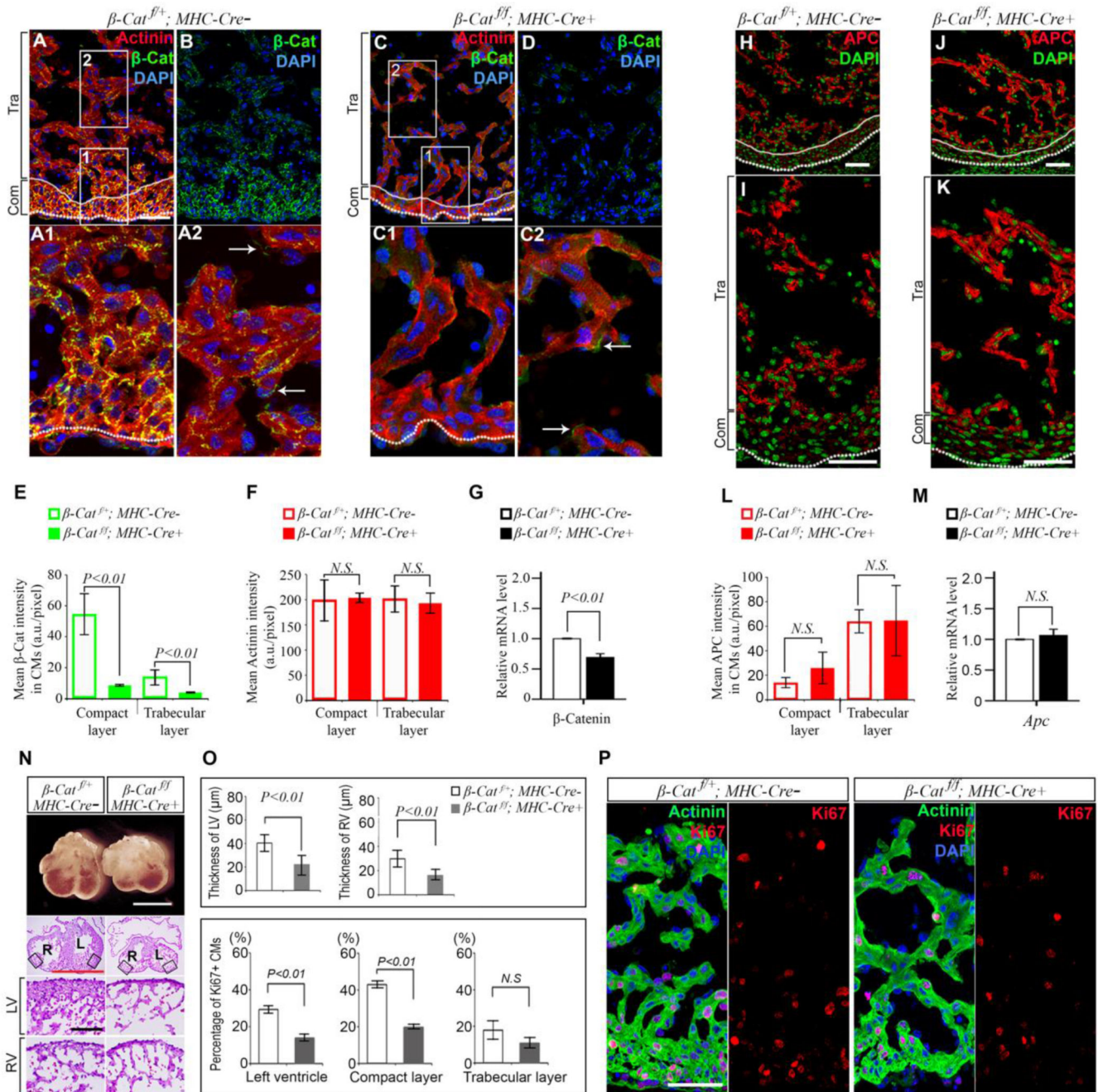
Figure 1.

Representative confocal images and quantitation of Wnt signaling and CM proliferation gradients in the ventricular wall of normal E13.5 embryos. A and B, β-catenin is stronger at the compact (Com) than trabecular (Tra) layer and quantitation of average β-catenin intensity (B, bar graph) in Actinin positive CMs that contain membranous and nuclear β-catenin (B). C and D, Ki67 gradient with low power view (C) and double labeling with sarcomeric α-actinin (Actinin, D) and quantitation of percentage of Ki67 (bar graph) positive CMs in Com and Tra layers. E and F, APC decorates Actinin positive CMs, but not

Actinin negative endothelial cells (triangles) and quantitation shows higher APC intensity in Tra than in Com layer. G, An illustration (left) shows how nuclear β-catenin intensity was measured for entire images as well as bar graphs demonstrate average nuclear β-catenin intensity in Com and Tra layers. Regions of interest (ROIs) are semi-automatically outlined by image J based on all Actinin positive areas. H, A diagram illustrates that β-catenin is expressed at the highest levels in the rapidly proliferating compact myocardium, forming a decreasing intensity gradient from the epicardium to the endocardium. In contrast, APC shows the strongest expression at the slowly proliferating trabecular layer form an increasing intensity gradient from the epicardium to the endocardium. Dotted lines show visceral pericardium and bars=50μm. Data represent mean ± SD. N=3-4 independent experiments.

Figure 2.
Cardiac deletion of β-catenin results in ventricular hypoplasia at E13.5. A and B, Double labeling of β-catenin and sarcomeric α-actinin (Actinin) in WT (A and B) and β-catenin (C and D) deleted hearts (*β-Cat* cKO) shows effective deletion of β-catenin in Actinin positive CMs and thinning of ventricular walls in *β-Cat* cKO hearts; Arrows indicated β-catenin signals from endothelial cells. E, Average β-catenin intensity is downregulated in Actinin positive CMs of *β-Cat* cKO hearts. F, Average Actinin intensity shows no difference between compact and trabecular layers or among WT and *β-Cat* cKO hearts. G, Real time

RT-PCR reveals downregulation of β-catenin mRNA levels in *β-Cat* cKO heart. H to K shows APC expression by confocal microscopy (H and J, lower power; I and K, higher power), average intensity (L) or real time RT-PCR (M). APC is mildly upregulated in *β-Cat* cKO hearts, but this change is not statistically significant. N, Cardiac morphology shows that *β-Cat* cKO mice have smaller hearts with thinner left (L) and right (R) ventricular walls compared to WT controls; Boxed regions are zoomed in adjacent images; Scale bars, 1 mm (white and red) and 100 μm (black). O, Ventricular wall thickness (upper panel) in *β-Cat* cKO and WT mice and percentage of Ki67 positive CMs (lower panel) in ventricular walls of *β-Cat* cKO and WT mice. P, Double labeling of Ki67 with Actinin. Data represent mean ± SD. N=3-4 independent experiments.
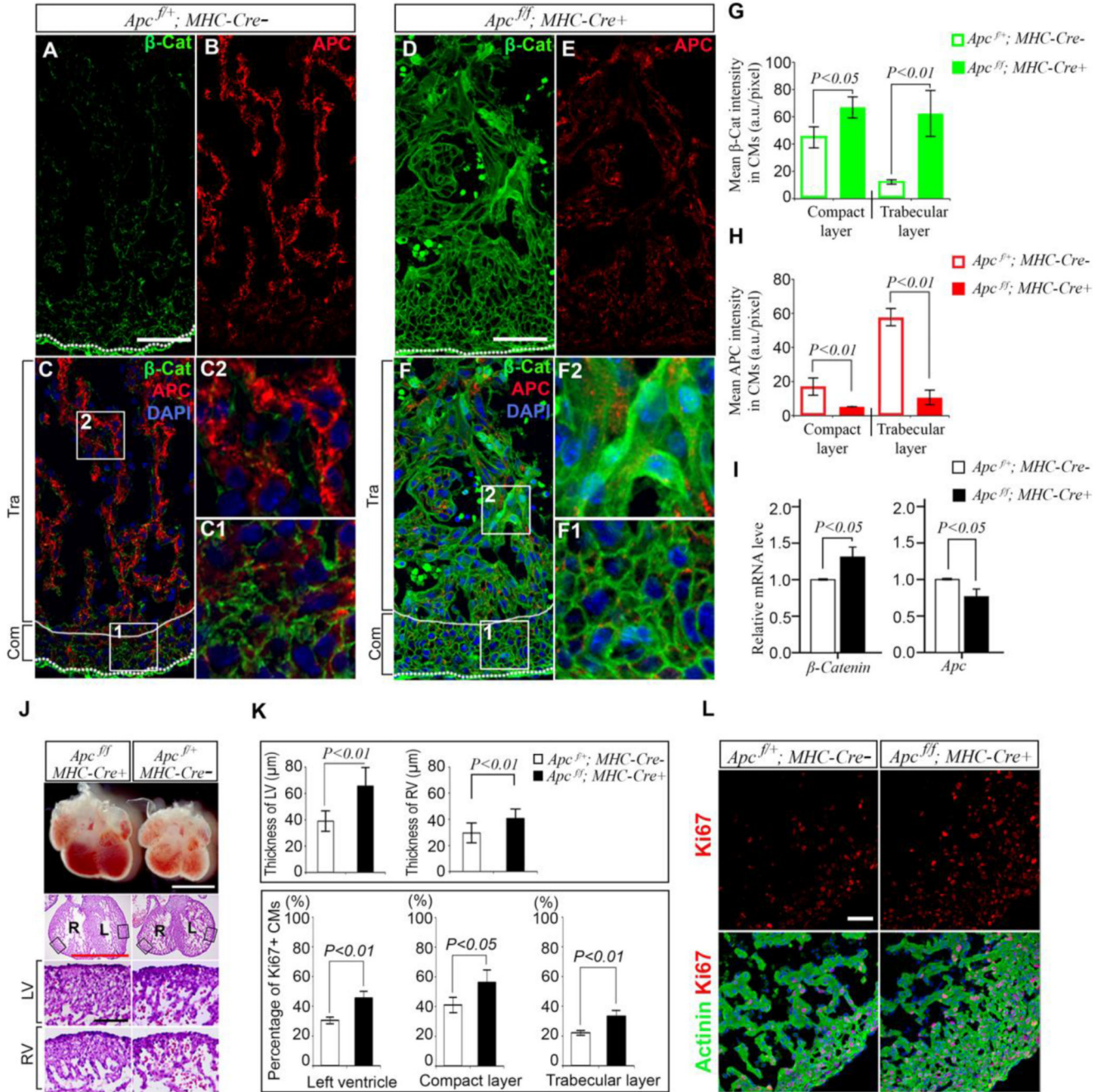
Figure 3.
Wnt activation by cardiac APC deletion promotes CM proliferation at E13.5. A to G, Double labeling of APC with β-catenin in WT (A-C) and *Apc* (D-F) deleted hearts (cKO) shows effective deletion of *Apc* and upregulation of β-catenin. G, Average β-catenin intensity is increased in *Apc* cKO hearts. H, Average APC intensity is decreased in *Apc* cKO hearts. I, Real time RT-PCR reveals downregulation of *Apc* and upregulation of β-catenin mRNA levels in *Apc* cKO heart. J, Cardiac morphology shows that *Apc* cKO mice have bigger hearts with thicker left (L) and right (R) ventricular walls compared to WT controls;

Boxed regions are zoomed in adjacent images; Scale bars, 1 mm (white and, red) and 100 μm (black). K, Ventricular wall thickness (upper panel) in *Apc* cKO and WT mice and percentage of Ki67 positive CMs (lower panel) in ventricular wall of cKO and WT mice. L, Double labeling of Ki67 with Actinin. Data represent mean ± SD. N=3 independent experiments.
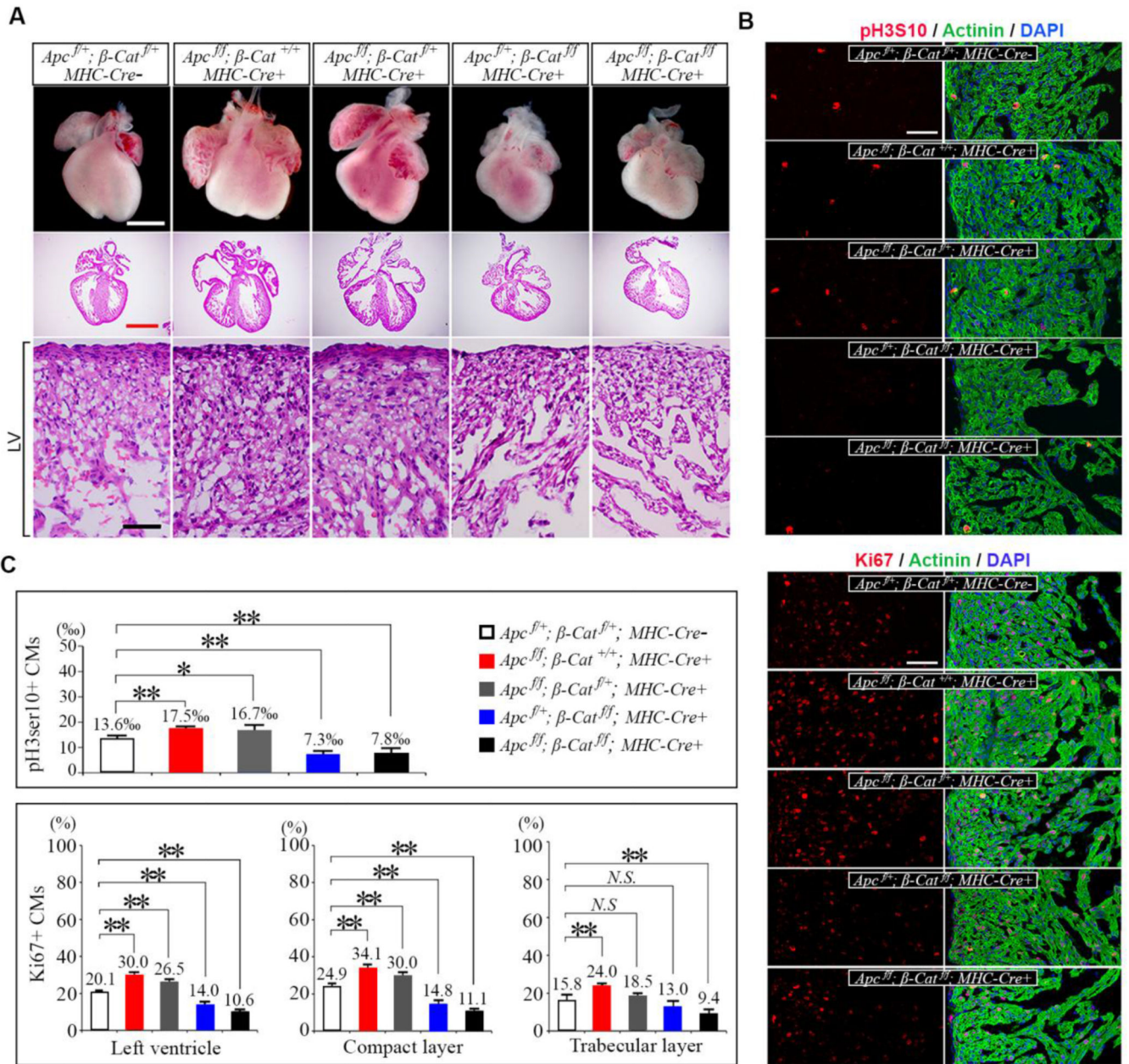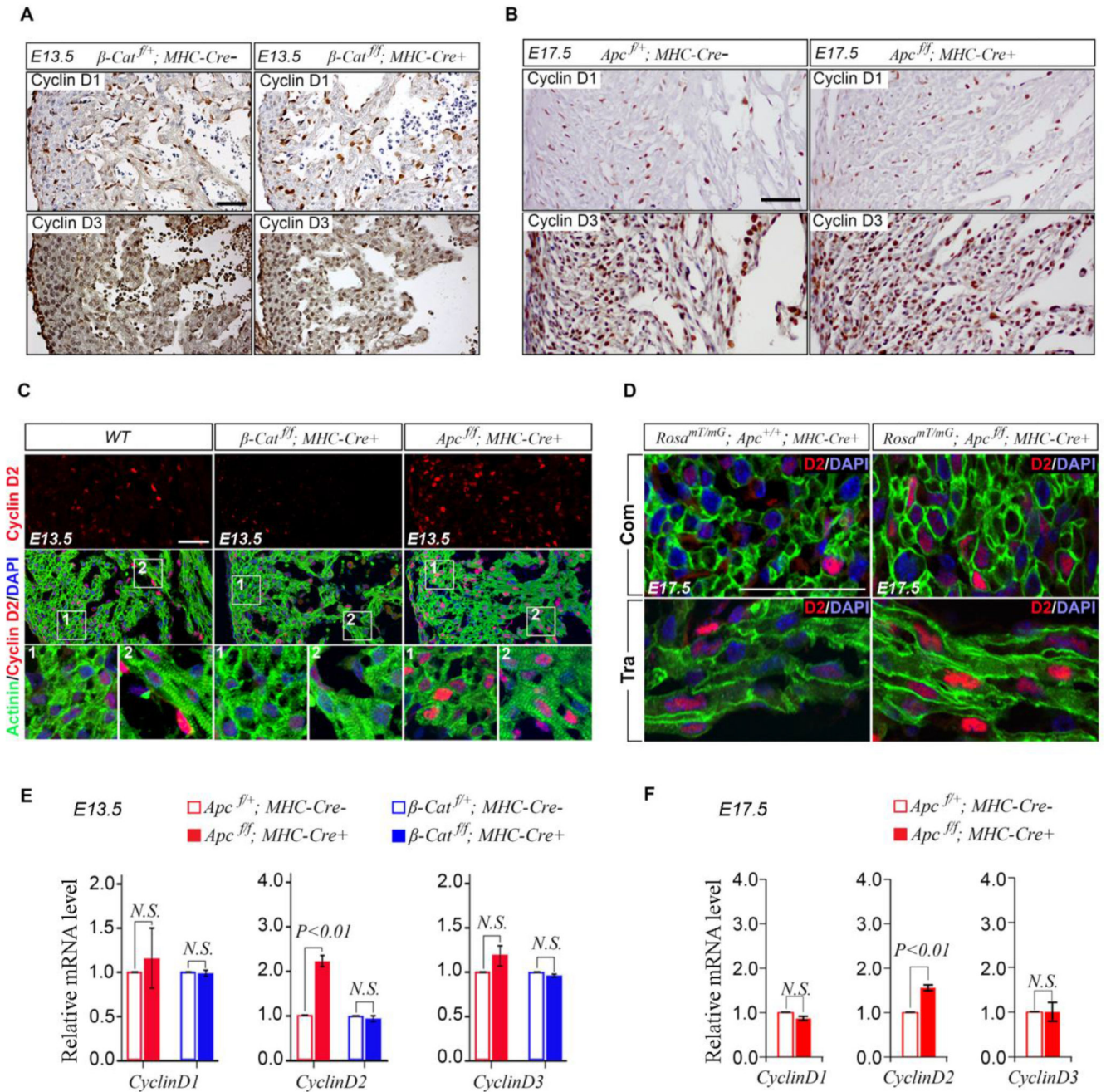
Figure 4.
Cardiac morphology and proliferation activity in compound *Apc* and *β-catenin* (*β-Cat*) deletion hearts at E17.5. A, Gross and H&E morphology of individual hearts with left ventricular walls zoomed in the bottom row. Scale bars, 1 mm (white and red) and 100 μm (black). B, pH3S10 or Ki67 co-stained with Actinin and DAPI. C, Percentage of pH3S10 and Ki67 positive CMs in *β-Cat* and *Apc* compound cKO mice at E17.5. Data are presented as mean ± SD from 3 to 4 embryos in each genotype. * *P*<0.05 and ** *P*<0.01 indicate statistically significant difference between the groups (ANOVA).

Figure 5.
Expression of D-type cyclins in E13.5 and E17.5 embryos. A and B, Cyclin D1 and cyclin D3 expression is not affected by either *β-catenin* (*β-Cat*, A, E13.5) or *Apc* (B, E17.5) deletion. Interesting, cyclin D1 is mainly expressed in endothelial cells while cyclin D3 is detected in both CMs and endothelial cells. C, Cyclin D2 is expressed in both CMs and endothelial cells and its expression increases in CMs of *Apc* cKO mice, but decreases in CMs of *β-Cat* cKO mice at E13.5. D, Cyclin D2 continues to increase in both compact and trabecular CMs that are deleted of *Apc* and contain membrane-targeted green instead of red fluorescent protein at E17.5. E and F, Expression of *cyclin D1, D2* and *D3* by real time RT-

PCR in cardiac *β-Cat* and *Apc* deleted hearts at E13.5 (E) and E17.5 (F). Scale bars= 50 μm. N=3-4 independent experiments.
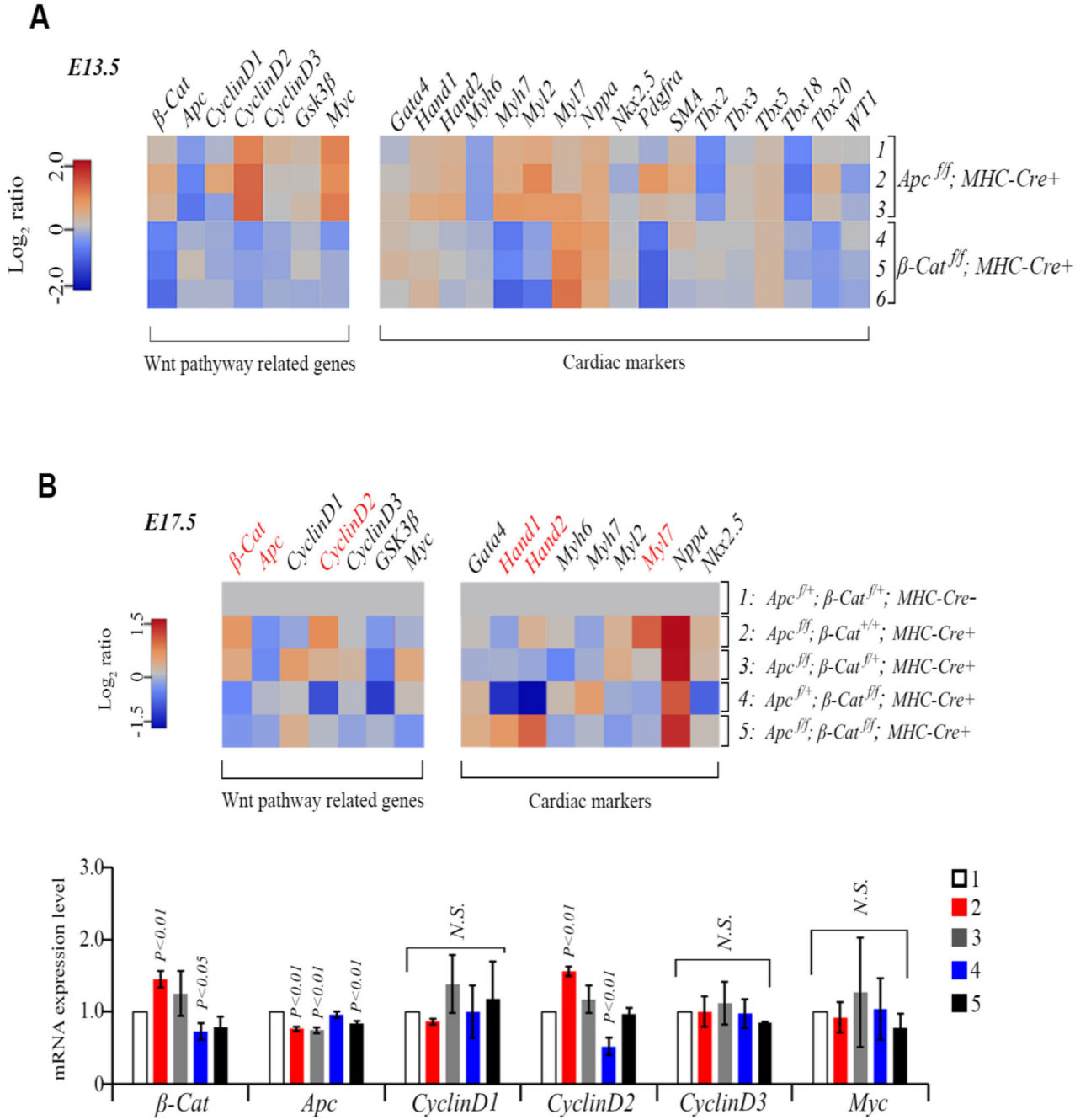
Figure 6.
Gene expression by real time RT-PCR in cardiac *β-catenin* (*β-Cat*) and *Apc* deleted hearts at E13.5 and E17.5. A, A heat map shows log2-fold changes of selective genes in *β-Cat* cKO and *Apc* cKO mice compared to their WT siblings. B, A heat map (upper) and bar graphs (bottom) reveal log2-fold changes of selective genes in compound *Apc* and *β-Cat* deletion hearts at E17.5. Post hoc multiple comparisons were performed in these target genes.

Targets with statistical significance among groups are marked in red. N=3-4 for each genotype. Each sample contains 3 technical replicates.